Pulsed laser deposition in Twente: from research tool towards industrial deposition

2014 J. Phys. D: Appl. Phys. 47 034006

(http://iopscience.iop.org/0022-3727/47/3/034006)

IOP Publishing Journal of Physics D: Applied Physics
J. Phys. D: Appl. Phys. 47 (2014) 034006 (8pp) doi:10.1088/0022-3727/47/3/034006

Pulsed laser deposition in Twente: from research tool towards industrial deposition

Dave H A Blank[1,2], **Matthijn Dekkers**[3] and **Guus Rijnders**[1,2]

[1] MESA+ Institute for Nanotechnology, University of Twente, PO Box 217, 7500 AE, Enschede, The Netherlands
[2] Twente Solid State Technology, PO Box 256, 7500 AE, Enschede, The Netherlands
[3] SolMateS BV Drienerlolaan 5, bldg 46, 7522 NB, Enschede, The Netherlands

E-mail: d.h.a.blank@utwente.nl

Received 25 July 2013, revised 12 November 2013
Accepted for publication 22 November 2013
Published 23 December 2013

Abstract

After the discovery of the perovskite high T_c superconductors in 1986, a rare and almost unknown deposition technique attracted attention. Pulsed laser deposition (PLD), or laser ablation as it was called in the beginning, became popular because of the possibility to deposit complex materials, like perovskites, as thin film. By introducing *in situ* diagnostics and control of the laser fluence, PLD became a technique for several experimental studies of diverse complex materials. Nowadays, first steps towards industrial applications of PLD thin films on large wafers, up to 200 mm, are underway. In this paper we give a brief overview of the progress that PLD has made in our research group in Twente. Starting with control of deposition parameters, via *in situ* diagnostics with reflection high-energy electron diffraction and ending with the latest development in equipment for large-area deposition.

Keywords: Pulsed laser deposition, surface diffusion, epitaxial growth, strontium compounds, oxygen compounds

(Some figures may appear in colour only in the online journal)

1. Introduction

Pulsed laser deposition (PLD) differs from other physical vapour deposition techniques because of the very high kinetic energy of the ablated particles arriving at the substrate and the high deposition rate during each laser pulse. Both influence the fabrication of thin films significantly, which can be used to manipulate the growth. For example, the effective diffusion coefficient of the colliding particles is direct depending on the kinetic energy of the ablated particles. Furthermore, high supersaturation can be used to accomplish layer-by-layer growth in a regime where usually island growth is observed. Another distinctive feature of PLD is the separation between deposition and growth. This makes it possible to study the as-grown material without being hindered by the deposition of new material. These studies have led to control of the growth of complex materials at the atomic level. As a result, PLD became very suitable for the fabrication of complex oxide thin films.

In physical vapour deposition techniques, like molecular beam epitaxy, most growth studies have been conducted with reflection high-energy electron diffraction (RHEED), basically an ultra-high vacuum analysis tool, thus in discrepancy with the relative high pressures during PLD of, e.g., complex oxides. The development of high-pressure RHEED gave us the ability to study the growth at relatively high pressures and has made it possible to establish growth control in PLD at the atomic level. It has made PLD, at present, an advanced research technique. However, achieving this atomic control is only possible when we use atomically flat, ideally well-controlled single terminated, crystalline substrates. Finally, for the use of PLD as a technique suitable for industrial applications up-scaling is essential. Although enormous progress has been made, still a number of important issues have to be resolved.

2. The renewed interest in PLD

PLD was a somewhat exotic deposition technique, until 1987. In that year the so-called high-temperature superconductor was discovered, after Bednorz and Müller discovered the perovskite superconducting LaBaCuO in 1986 [1]. This complex oxide material could be synthesized in bulk by solid-state reaction or, more homogeneously, by chemical routes. One of the purest phases of the YBaCuO powder can be obtained with the citrate synthesis followed by a pyrolysis procedure, as published by Blank *et al* [2]. The discovery of a superconductor that shows superconductivity above the boiling temperature of liquid nitrogen has started a massive research effort towards the thin-film fabrication of this perovskite material. Several issues became important, like thin-film growth in an oxygen background with relative high oxygen pressures. Hammond and Bormann [3] published, very soon after the discovery of the high-T_c superconductor, a phase diagram wherein the importance of temperature and oxygen pressures is given to obtain the correct phase. The search towards a deposition technique, where oxide thin films with complex stoichiometric ratios could be fabricated at relatively high oxygen pressures and temperatures, resulted in a renewed interest in PLD. Dijkamp *et al* [4] showed the applicability of this overlooked technique. After these first published results many groups show improved results and PLD became a popular technique in several laboratories all over the world. Nowadays PLD has become the deposition method to fabricate and study, in a research laboratory environment, epitaxial and single crystalline thin films of complex oxides, like superconducting high-T_c cuprates, metaloxides, and ferroelectric, ferromagnetic, and dielectric oxides. The success of PLD is due to the fact that it is conceptually as well as operationally a relatively simple technique. A high-energy pulsed laser beam is focused on a target, causing evaporation (ablation) of material with the same stoichiometric ratio as the target is made from. The highly energetic material (plasma) is deposited on a substrate leading to thin-film growth.

One distinctive property of PLD is the pulsed nature of deposition. Just after the laser pulse deposition of material takes place within a very short time frame, typically a few microseconds. While in between the pulses most of the film growth takes place. This allows growth to be studied without being disturbed by deposition of new material. Furthermore, the short duration of intense deposition results in a high supersaturation affecting the nucleation and growth processes. It has been shown that for different deposition conditions the mean diffusion time of adatoms, given by the activation energy for diffusion and the growth temperature, can be as long as several seconds. Therefore, the two basic processes, i.e. random deposition and growth through rearrangements are separated in time (see figure 1 for a schematic view). This separation enables us to study the diffusivity and other kinetic parameters during growth.

To study the surface morphology and thin-film growth, most often RHEED is used. Intensity oscillations of the specular electron beam as well as the diffraction pattern due to the interaction of the high-energy electrons with the crystal surface give important information on the thin-film growth. Therefore, it was obvious to introduce RHEED in PLD as well. However, this is not a trivial operation. As mentioned before, the success of PLD is the possibility of a relatively high (oxygen) pressure during deposition combined with the high energetic plasma particles. Both are affected by the electron beam and to use RHEED during PLD it was necessary to modify the set-up.

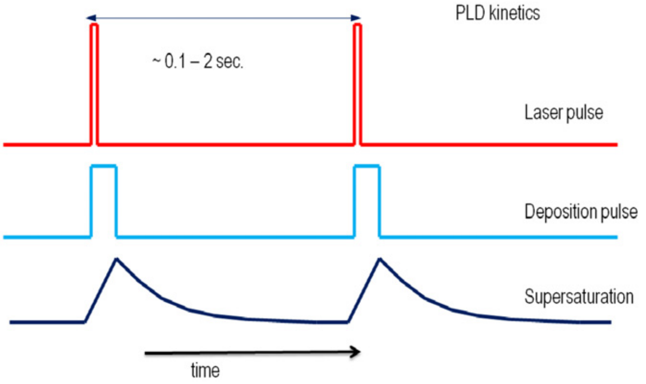

Figure 1. Schematic view of pulsed laser deposition, in which the deposition and growth are separated in time. The laser pulse is typically 50 ns. The laser pulse initiates a plasma of ablated particles, that exists for several hundred microseconds. The third phase is the actual deposition of supersaturated material on a substrate, where nucleation and growth takes place without any disturbance of new ablated material. Monitoring of this decay by *in situ* RHEED enables measurement of the kinetic parameters at growth conditions.

3. *In situ* diagnostics with RHEED during PLD

After the introduction of RHEED this surface-sensitive technique was primarily used for the study of cleaved crystal surfaces and surface reconstruction. Nowadays, RHEED is mostly used to monitor growth and study growth kinetics. The RHEED oscillations [5], derived from the variation of the intensity of the scattered beam of the electrons on the deposited material provides important information about the different growth mechanisms. If the intensity of the specular beam varies in a periodic way this is a signature for layer-by-layer growth, damped oscillations during deposition, most probably layer-by-layer followed by island growth occurs and no oscillations with high intensity is a signature for step flow, or no oscillations with diffuse specular spot is indicating surface roughness or amorphous growth. Of course, RHEED oscillations are an excellent indicator to verify and determine the growth rate. To make use of RHEED during PLD of complex oxides, where the background pressure is relatively high, the elastic and inelastic electron scattering has to be minimized and, on the other hand, a low pressure is required near the filament in the electron gun. To overcome this dilemma, a differential pumped e-gun was introduced by Karl and Stritzker, which makes it possible to use deposition pressures and RHEED analysis to about 1 Pa [6]. This pressure is still too low to fulfil the requirements for the growth of stable phases of many complex oxides or to achieve a required growth mode, like layer-by-layer or step flow.

3.1. High-pressure RHEED set-up

The idea of high-pressure RHEED is two-fold. First a low pressure in the e-gun, secondly, a short travelling distance of

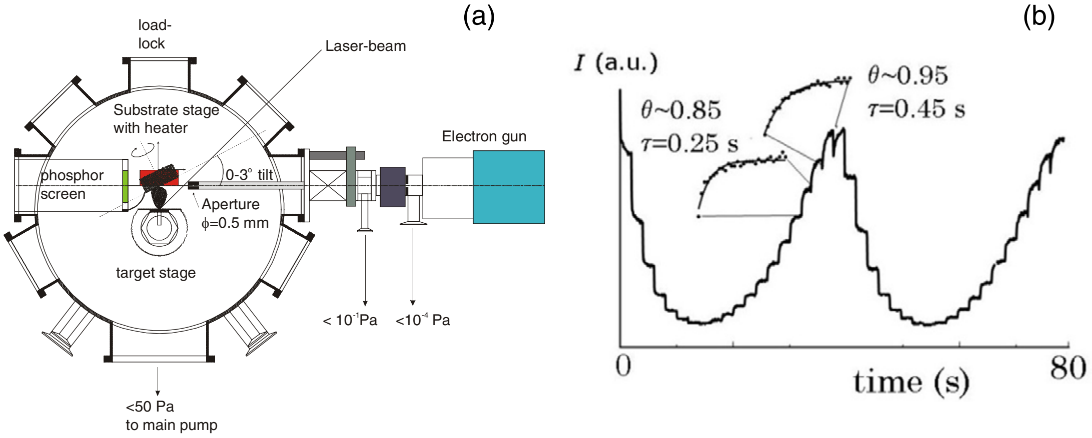

Figure 2. Schematic view of our PLD system equipped with high-pressure RHEED (*a*). Real-time observed intensity of the specular reflected RHEED spot during deposition at 750 °C of two unit cell layers of $SrTiO_3$ (*b*). The insets show the relaxation of the intensity due to growth, where O is the convergence and τ the relaxation time of the deposited material. (Reprinted from [7].)

the electrons at high pressures. The latter holds for the distance from electron gun towards the substrate as well as the distance between the substrate and phosphorous screen, where the specular beam becomes visible. To satisfy these requirements a two-stage differential pumped RHEED system was designed [7]. A schematic sketch of the designed high-pressure RHHED PLD system is given in figure 2(*a*). The e-gun (EK-2035-R, STAIB Instrumente) has a minimum beam size of ∼250 μm (FWHM) up to a working distance of 500 mm. The gun is attached to a flange in which a stainless steel extension tube with an inner diameter of 8 mm is mounted. A differential pumping unit is used to preserve a vacuum of better than 10^{-4} Pa in the e-gun. An aperture (diameter 0.5 mm) separates the tube from the deposition chamber. The pressure in the tube, of course depending on the pump speed and the size of the aperture, is in our case kept below 10^{-1} Pa. Using this two-stage pumping system, the pressure in the deposition chamber can be increased up to 100 Pa maintaining the low pressure in the electron source. The e-beam, which passes through the apertures inside the differential pumping unit and the tube, enters the deposition chamber near the substrate at a distance of 50 mm. The *XY* deflection ability of the electron source, which is a standard feature for e-guns, is in this case used to adjust the e-beam through the aperture at the end of the tube. The electron source, including the extension tube, is mounted on an *XYZ*-stage allowing adjustment of the distance between substrate and end of the tube. This extension tube reduces the travelling distance of the electrons in the higher pressure regime to 100 mm. Here the intensity losses inside the tube, with pressure below 10^{-1} Pa, are negligible, whereas the scattering losses inside the chamber are significant. At oxygen pressures of PO_2 ∼100 Pa, the intensity will drop to 1% of the initial intensity of the electrons in the gun. Nevertheless, the scattering losses can be compensated by adjusting the e-beam current. This leads to a visible and detectable reflected specular spot up to oxygen pressures of about 50 Pa, a pressure regime that is most favourable for the growth of high-quality complex oxide thin films. With this high-pressure set-up it is possible to follow the growth during deposition, as a growth monitor system, but also to study the growth behaviour of these complex materials.

3.2. Growth studies with high-pressure RHEED

From the very first experiments, done with high-pressure RHEED during the deposition of homoepitaxy of $SrTiO_3$, it became clear that the RHEED pattern provided an overwhelming amount of information. This holds for the growth mode, but, most interestingly, also for the diffusivity of the deposited material. Due to the earlier mentioned separation in time of the deposition and growth of the material it became possible to look to the relaxation behaviour of the high-supersaturated deposited material. In figure 2(*b*) the specular RHEED intensity is given during the deposition of $SrTiO_3$ at substrate temperature of 750 °C with an oxygen background pressure of 3 Pa. The clear intensity oscillations show that, under these growth conditions, 2D nucleation or layer-by-layer growth takes place. The period of one oscillation corresponds to the growth of one unit cell of $SrTiO_3$. The full recovery of the intensity indicates an ideal layer-by-layer growth. The pulsed deposition leads to modulation of the RHEED intensity. During each pulse, in this experiment, about 6% of a unit cell is deposited on the substrate within a few hundred seconds. The mobility of the deposited material leads to a relaxation of the RHEED intensity after each pulse. From this relaxation, the diffusivity of the deposited material can be followed. From figure 2(*b*) it can be seen that time constants are measured up to 0.45 s. This relaxation is due to the mobility of the deposited material that diffuses towards the step edges of the grown islands. This causes the islands to grow and, consequently, a change in the step density. The change of the step density after every pulse leads to a decay of the density of the diffusing particles, which depends on the diffusivity and the average travel distance. This distance is determined by the nucleation density and the average island size. The latter depends on the coverage and causes the coverage characteristic relaxation times, see figure 2(*b*). In [8] an in-depth discussion of this behaviour is given. One consequence of this relaxation behaviour at relatively high background pressures, compared to the low pressures with other physical depositions techniques, is the possibility for, e.g., growth manipulation to achieve 2D-growth of complex materials at conditions where standard deposition leads to island growth.

3.3. Growth manipulation

Controlling the growth during PLD using high-pressure RHEED makes it possible to grow heterostructures and multilayers with atomically smooth interfaces. Here, layer-by-layer growth is a prerequisite and 3D island formation has to be avoided. An option could be step-flow growth, because in that case the roughness of the grown film does not exceed one unit cell layer. In this case the RHEED intensity will be steady, so no oscillations are visible and consequently no information about the deposition rate can be obtained. Usually, during the deposition of complex materials, roughening of the surface takes place. Due to a lack of diffusivity or limited interlayer mass transport of the deposited material at the substrate surface, nucleation takes place on top of 2D islands before a complete unit cell layer has been realized. This is causing roughness, which can hamper the applicability in multilayer structures and device applications. It is important to avoid this roughening, which can be realized by making use of the high supersaturation of the deposited material and the diffusion relaxation at the desired temperature and background pressure. Increasing the laser repetition rate, so decreasing the time between the pulses, the high supersaturating can be maintained. If the deposition rate during one laser pulse is known, one can calculate the number of pulses needed to complete one unit cell layer. If one succeeds in depositing this amount of material (total number of pulses) with high laser frequency followed by no deposition, the supersaturation and therefore high nucleation density will lead to a closed, and thus a smooth, layer. This growth method, which can easily be achieved with PLD, makes it possible to grow in layer-by-layer mode in a growth regime (temperature, pressure) where otherwise 3D island formation would dominate the growth [9]. In figure 3 the results of this so-called pulsed laser interval deposition the effect of the interval deposition is shown. Here, the standard deposition of homoepitaxial growth of $SrTiO_3$ at 10 Pa and at deposition temperature of 800 °C leads to a decrease of the specular spot RHEED intensity each unit cell that is deposited, figure 3(*a*). This is caused by an increase of surface roughness, as seen by the left atomic force microscopy (AFM) image taken from a 30 nm thick $SrTiO_3$ film, figure 3(*e*). From the first RHEED oscillation one can calculate the number pulses that are needed to complete a full unit cell layer. In this example this will be 27 pulses, figure 3(*d*). By depositing these 27 pulses at a higher deposition rate, followed by a period without deposition, a complete unit cell layer is formed, figure 3(*b*). As a result, the film roughness of a 30 nm thick film, made by interval deposition shows only unit cell steps, figure 3(*f*). The imprint of the substrate step edges is clearly visible after 80 intervals. In figure 3(*c*) the difference between the maximum intensity of the specular spot is given of a continuous growth and interval deposition: the higher the intensity, the smoother the thin film.

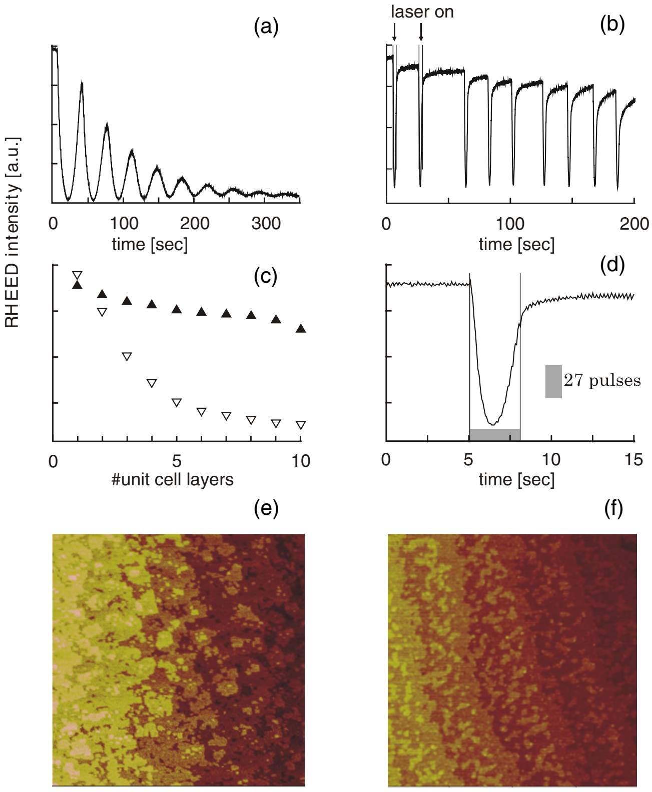

Figure 3. Specular RHEED intensity recorded during homoepitaxial growth of $SrTiO_3$ at 10 Pa and 800 °C using 'standard' PLD (*a*) and interval PLD (*b*). Intensity maxima using 'standard' PLD: ▽ and interval PLD: ▲ (*c*). Intensity variation during one deposition interval (*d*). The surface morphologies of ∼ 30 nm thick $SrTiO_3$ films are depicted in the AFM micrographs (1 μm^2): 'standard' PLD (*e*) and interval PLD (*f*). (Reprinted from [9].)

4. Single terminated substrates

For epitaxial layers, it is necessary to start with crystalline substrates with, in a number of cases, a singly terminated atomic plane. Moreover, the above shown RHEED data and growth manipulation was only possible with atomically smooth surfaces. The (pseudo)cubic unit cell of a perovskite (ABO_3) oxide can be represented as a multilayer of alternating AO and BO_2 in the [0 0 1] direction (figure 4(*a*)). After cleaving a single crystal, both terminations are expected at the surface in equal proportion, resulting in mixed terminated surfaces with steps of half or one unit cell height (0.2 nm and 0.4 nm, respectively) (see figure 4(*b*)). Although these surfaces can be considered as atomically flat, this mixed termination influences the growth, e.g. island formation, significantly. From RHEED studies it became clear that single termination (see figure 4(*c*)), is essential for controlled growth at an atomic level. The typical surface treatment of perovskite-type oxides that includes high-temperature annealing which results in ordered, well-defined, crystalline surfaces, showed still mixed termination and therefore inadequate. Kawasaki *et al* introduced wet etching of $SrTiO_3$ (0 0 1), which was the first important step towards singly terminated perovskite-type surfaces [10]. By etching the surface with an acidic NH_4F buffered HF solution (BHF) they obtained a TiO_2 terminated surface, as confirmed by ion scattering spectroscopy. To obtain

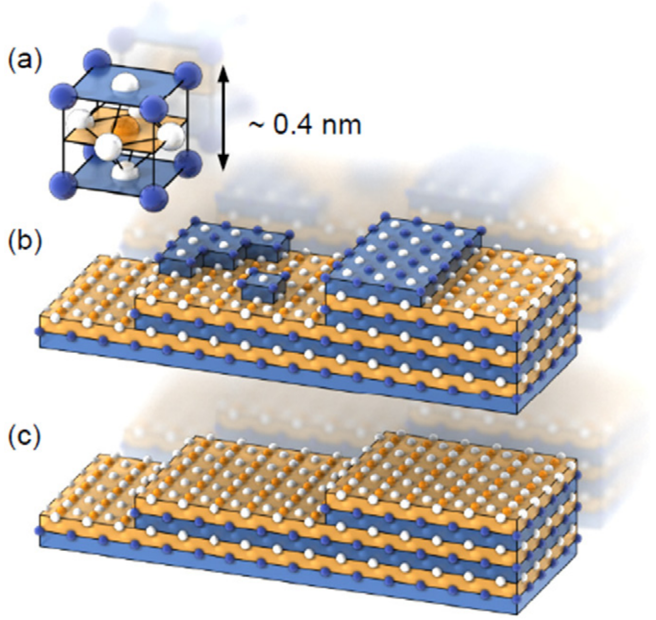

Figure 4. The ABO_3 unit cell, where A is typically a rare-earth, alkaline earth or alkali metal ion, and B is often a transition metal ion (*a*). A schematic representation of a mixed terminated surface with steps of 0.2, 0.4 and 0.6 nm high (*b*). A single terminated BO_2 surface with steps of 0.4 nm high (*c*). The blue blocks correspond to the AO layer and the yellow blocks to the BO_2 layer with blue, yellow and white circles corresponding to A, B and O ions, respectively.

single termination, the pH of the etchant is claimed to be crucial to achieve selectivity. However, since the treatment severely depends on the $SrTiO_3$ surface quality prior to etching, this method often leads to uncontrolled wet etching. To etch $SrTiO_3$ in a controlled manner Koster *et al* introduced the formation of an intermediate Sr-hydroxide complex by immersion in water [11]. The method is based on expanding the difference in selective etchings of the different termination layers, in this case between SrO or Sr-hydroxide and TiO_2. By subsequent short BHF etching, reproducible TiO_2 terminated surfaces were obtained. Currently, this method is expanded to $SrTiO_3$ (1 1 1) by removing SrO_x, giving a Ti terminated surface [12, 13]. This idea of expanding the difference in etchings can be applied to many other perovskite substrates. Although $SrTiO_3$ is the most used substrate in oxide electronics, other substrates are also gaining interest for better misfit or to achieve strain during growth [14]. Frequently used substrates in complex oxide devices are $LaAlO_3$, $NdGaO_3$, LSAT (ranging from lattice parameter 3.8 Å to 3.9 Å and the scandates $DyScO_3$, $GdScO_3$ and $NdScO_3$, with lattice parameter ranges from 3.94 Å to 4.02 Å. Nowadays, for almost all perovskite substrates a treatment has been developed to achieve single termination. For the atomically defined rare-earth scandate crystal surfaces, we refer to Kleibeuker *et al* [15].

5. Oxide electronics

The perovskite oxide compounds are interesting for oxide electronics because these complex oxide materials show various properties, with similar crystal structures and lattice parameters. By changing the atoms in the structure, perovskites can exhibit ferroelectricity, ferromagnetism, superconductivity, piezoelectricity, colossal magnetoresistance or high dielectric permittivity. The growth studies of complex oxides using RHEED resulted in atomic accuracy during deposition and atomically flat and well-defined interfaces. The treatment of substrates results in single termination with the control of electronic properties with nanoscale precision [16, 17]. Due to the small lattice match between these perovskites, multilayers can be grown epitaxially. Even so, a small lattice mismatch does not have to be a disadvantage, because strain can be beneficial for the desired properties by modifying the ferroelectricity, ferromagnetism, superconductivity, piezoelectricity, colossal magnetoresistance and high dielectric permittivity of perovskite oxides [18–21]. With the above-mentioned control on an atomic level, layer-by-layer or block-by-block growth is possible. It opens the way to devices with novel functionalities [22]. An example is the deposition of two materials with almost opposite properties, like ferroelectricity and ferromagnetism. Multilayers by alternating depositing both materials, e.g. in different sequences, can lead to artificial multiferroics. Besides novel ‘bulk’ properties of these artificial layers, the interface becomes increasingly important. Devices that rely on interface properties have already been realized and exploited, like Josephson junctions and SQUIDs, magnetic tunnel junctions, or FeRAMS. However, this is only the beginning of the realization a complete class of oxide devices, based on controlled interfaces. It is expected that interfaces and surfaces in highly correlated systems are more promising than interfaces in conventional metals and semiconductors, but on the other hand are more complex. For example, interfaces break the translational and the rotational symmetry and induce stress or strain. Consequently, altering the distances and bonds between the ions gives rise to shift and distortion of the electronic states and energy levels and modifying the bands. The interfaces influence directly the electronic correlation and, thus, the electronic behaviour of the deposited multilayer. It opens the way to manipulate electronic and/or magnetic properties of these multilayers and leads the way to new types of devices.

A worthy example is the realization of atomically controlled interfaces between epitaxial heterostructures of

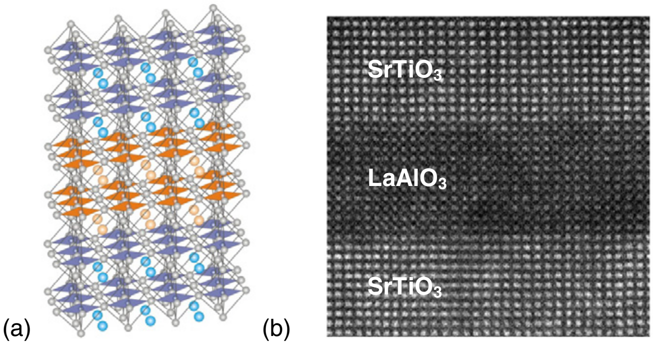

Figure 5. Schematic view of a $SrTiO_3/LaAlO_3/SrTiO_3$ heterostructure (*a*). Cross-section high-angle annular dark field (HAADF) TEM image of the $LaAlO_3/SrTiO_3$ superlattice along the [0 0 1] zone axis (*b*).

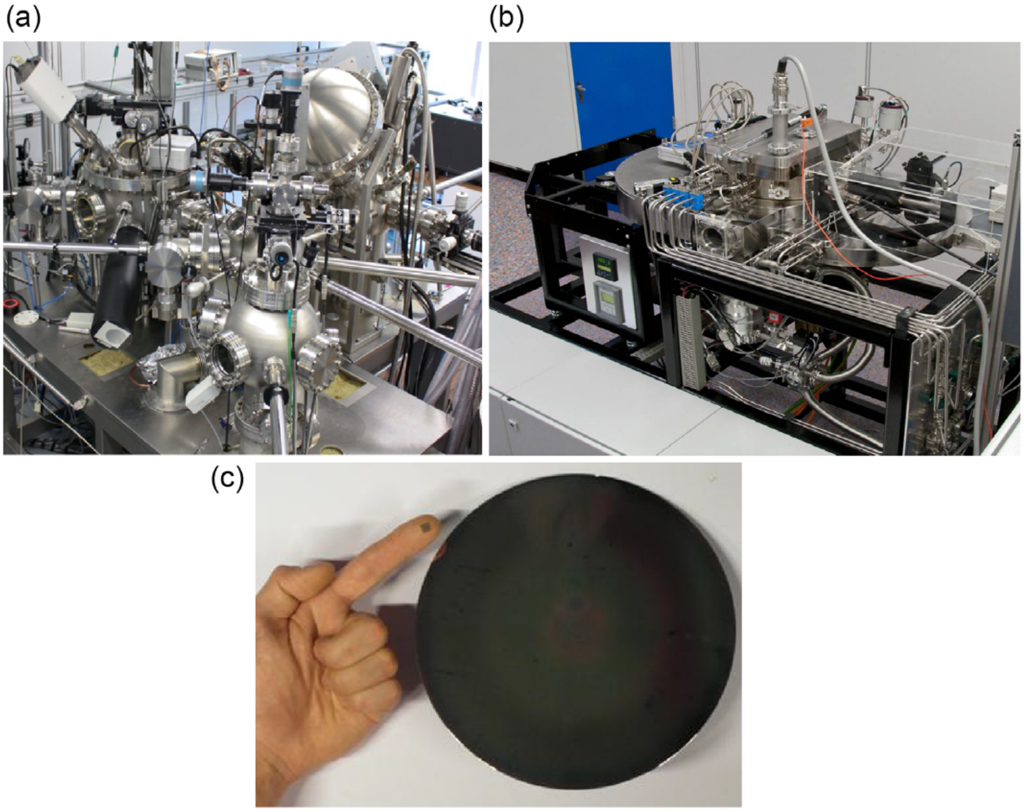

Figure 6. Scaling the synthesis of nanomaterials: from 5 × 5 mm^2 to 200 mm wafer size. On the right the TSST research system (*a*), on the left the Piezoflare of SolMateS (*b*). In (*c*) the difference is shown between the deposition areas of the research tool compared to the large-scale industrial deposition.

$SrTiO_3$ and $LaAlO_3$, both band insulators. In figure 5, a schematic view, figure 5(*a*), and a cross-section transmission electron micrograph (TEM), figure 5(*b*), are shown of a $SrTiO_3/LaAlO_3/SrTiO_3$ heterostructure, fabricated by PLD. RHEED is used to control the growth, which provided heterostructures with atomically defined interfaces, in this case $SrO–AlO_2$ or $TiO_2–LaO$. The conducting behaviour of the interface between the band insulators $SrTiO_3$ and $LaAlO_3$ have been seen as a consequence of the polarity discontinuity across the nonpolar/polar interface between $SrTiO_3$ and $LaAlO_3$ is caused due to the prevention of a so-called polar catastrophe [16, 17, 23]. In this case, a build-up of electric potential within the $LaAlO_3$ would generate transfer of electrons from the $LaAlO_3$ surface, through the $LaAlO_3$ layer, into the $SrTiO_3$ conduction band. This has been seen with a $LaAlO_3$ film thickness above a certain threshold of 3–4 unit cells [24]. An extra $SrTiO_3$ capping layer prevents structural and chemical reconstructions at the $LaAlO_3$ surface and results in metallic behaviour below this threshold, even down to a single $LaAlO_3$ unit cell layer [25, 26].

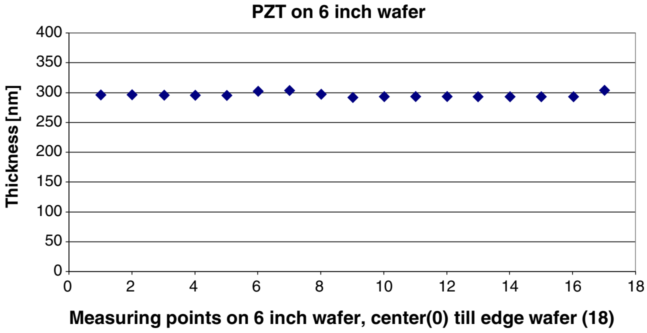

Figure 7. Thickness uniformity on 150 mm wafer of PZT, deposited at 550 °C. The average thickness is 297 nm (max 305 nm and min 293 nm).

Nevertheless, high-quality devices based on the above-mentioned conducting interfaces requires enhanced mobilities. One important aspect is to reduce the number of activated carriers and to further enhance the mobility. Here, new concepts and preparation routes are necessary. In this respect, PLD with modified deposition procedures, like interval deposition, can play an important role. An example is given in the paper of Huijben *et al* where it is shown that incorporation of a strontium copper oxide nanolayer strongly reduces the impurity scattering at conducting interfaces in oxide $LaAlO_3$–$SrTiO_3$(0 0 1) heterostructures, opening the door to high carrier mobility materials [27].

6. Industrial large-area PLD

In the previous paragraphs, it has been shown that PLD is a very versatile technique for the controlled synthesis of functional materials, including complex oxide and nanostructured films, nanowires, nanopillars, thermo-electric and artificial materials. These achievements have made PLD today's most advanced method for synthesizing thin films on small-scale areas.

When only a small area and a small number of samples are required, PLD can be considered as indispensable due to

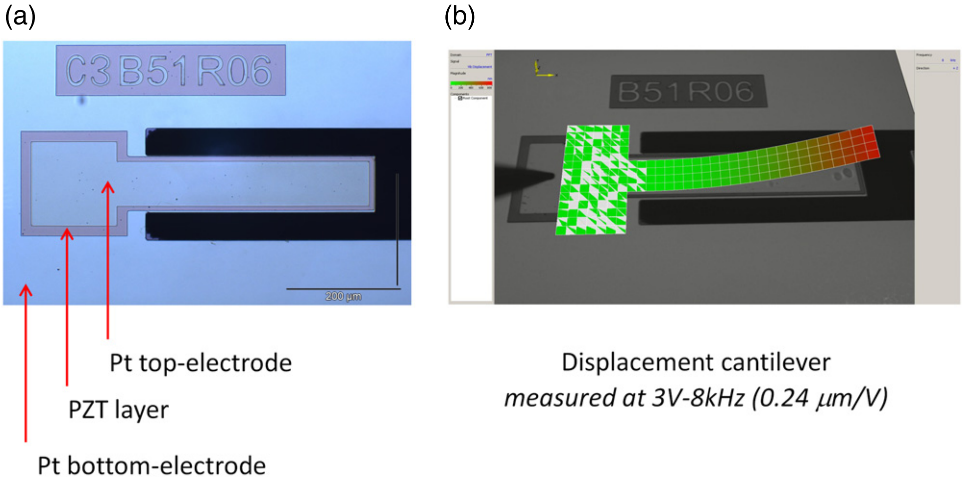

Figure 8. The cantilever structure obtained with deposited PZT on a 150 mm wafer by MEMS technology. The length of the cantilever is 400 μm (*a*). In (*b*) the displacement of the cantilever is given as measured by the laser Doppler velocimetry (LDV) at 3 V and 8 kHz (0.24 μm V^{-1}).

its superior control and precision of growth and synthesis. For many applications in for example nanoelectronics and photonics, energy, nanobiotechnology and nanomedicine it is highly desired to make such advanced level of control available for the industrial synthesis of thin films. However, until recently PLD could not meet the industrial needs for the synthesis of thin films because the area of controlled growth was typically restricted to a square centimetre with rather low deposition rates. The up-scaling of PLD was a major challenge. The reason is that nanoscale precision has to be maintained, over much larger areas and at higher deposition rates. Therefore, a scaling of PLD requires a fundamentally and quantitatively unprecedented understanding and control of the laser–target interaction, the dynamics of the ablation plasma, and the growth of nanomaterial films.

In academic laboratory systems, PLD including (high-pressure) RHEED thin-film fabrication with atomic precision is available nowadays. However, such fabrication can so far be achieved only with small samples, see figure 6(*a*). The reason for these limitations is the fact that the synthesis requires a strict control of the growth conditions and plasma parameters with great spatial homogeneity.

Recently, large-area deposition with PLD became available, able to grow thin films on wafers, up to 200 mm diameter, see figure 6(*b*). Here, the laser beam is homogenized, beam shaping and steering are included together with target and substrate manipulation. This has led to PLD systems, like the PiezoFlare 1200 (SolMateS) which has been designed to support seamless transfer of the developed processes to pilot or volume production. This PiezoFlare system is a fully automated, semi-compliant, single wafer deposition system up to 200 mm wafers. These systems are used for high-speed deposition of thin films such as piezoelectric Pb(Zr,Ti)O_3 (PZT) for micro-electronical–mechanical systems (MEMS) applications, ionic conducting YSZ for fuel cells or transparent electrical conducting layers on sensitive substrates, like flexible displays and OLEDs. In figure 6(*c*) the difference is shown between the deposition areas of the research tool compared to the large-scale industrial deposition.

In figure 7 the thickness uniformity of PZT deposited at 550 °C on a 150 mm wafer is given. The average thickness is 297 nm with a maximum of plus or minus 10 nm is achieved. Depositing PZT layers on a 150 mm wafer for use in Piezo MEMS shows the progress that has been made with large-scale deposition. In figure 8(*a*) a cantilever structure is shown with a PZT layer sandwiched between Pt electrodes. In figure 8(*b*) the displacement of this cantilever is measured with laser Doppler velocimetry. In figure 9 the piezoelectric properties is given from cantilevers, with increased cantilever lengths, that are positioned on different areas on the 150 mm wafer (at the centre and near the border of the wafer).

7. Epilogue

Although tremendous progress has been made in large-area PLD, up-scaling of the synthesis of thin films with perfect control over the structure and composition of the material at the atomic scale in a pilot line delivering large wafer size substrates with high throughput is still challenging. If this becomes feasible depends on different research topics that have to be fulfilled. Among them are the incorporation of novel high-power, high repetition rate lasers for record-speed target ablation, which will enable new deposition strategies based on state-of-the-art large-area PLD and involve advanced beam, target and substrate manipulation. Furthermore, to maintain precision at the atomic level, one has to employ *in situ* diagnostics of the transient dynamics of the laser-induced plasma plume with regard to atomic or molecular species and their flow. It is this transient dynamics, which physically relates the externally controllable scaling parameters (such as the intensity distribution, pulse duration, repetition rates and deposition geometries) to the growth of the film.

Additional theoretical modelling and monitoring of the dynamics of the growth kinetics (with a very high time resolution down to the microsecond) is needed to complete the understanding of the relation between material flow and film growth. Essential to this is the development of *in situ* plasma diagnostics, and *in situ* large-area growth and film diagnostics

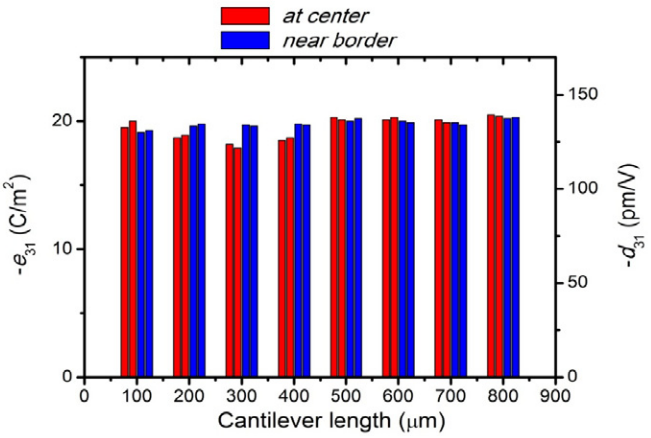

Figure 9. Relationship between piezoelectric e_{31} and d_{31} coefficients and cantilever length (cantilever width: 100 μm) in the centre and near the border of 6 inch SOI wafer.

allowing direct correlation with and control over the thin-film growth. Finally, for a full control of the material structure and composition during deposition, the diagnostics has to be implemented, together with feedback on the ablation process, the material flow in the plasma plume, and the substrate and target manipulation.

To conclude, important improvements have been made in the deposition of complex materials, like PZT. Nowadays wafer sizes up to 200 mm are feasible. The next step is to have full control of the laser characteristics and include plasma diagnostics to achieve control of the deposited materials on an atomic level, a prerequisite to make use of all the prosperity of complex oxides. PLD has developed from a small-scale research tool towards an industrial deposition technique.

Acknowledgments

We would like to acknowledge all (previous) members of the Inorganic Materials Science at the University of Twente, Netherlands, in particular Gertjan Koster, Mark Huijben and Josée Kleibeuker for their contributions.

References

[1] Bednorz J G and Muller K A 1986 *Z. Phys.* B **64** 189
[2] Blank D H A, Kruidhof H and Flokstra J 1988 *J. Phys. D: Appl. Phys.* **21** 226
[3] Hammond R H and Bormann R 1989 *Physica* C **162** 703
[4] Dijkamp *et al* 1987 *Appl. Phys. Lett.* **51** 619
[5] Neave J H *et al* 1983 *Appl. Phys.* A **31** 1
[6] Karl H and Stritzker B 1992 *Phys. Rev. Lett.* **69** 2939
[7] Rijnders G, Koster G, Blank D H A and Rogalla H 1997 *Appl. Phys. Lett.* **70** 1888
[8] Eason R (ed) 2008 *Pulsed Laser Deposition of Thin Films* (New York: Wiley) ISBN 0470052120
[9] Koster G, Rijnders G, Blank D H A and Rogalla H 1999 *Appl. Phys. Lett.* **74** 3729
[10] Kawasaki M *et al* 1994 *Science* **266** 1540
[11] Koster G, Kropman B L, Rijnders G, Blank D H A and Rogalla H 1998 *Appl. Phys. Lett.* **73** 2920
[12] Chang J, Park Y S and Kim S K 2008 *Appl. Phys. Lett.* **92** 152910
[13] Biswas A *et al* 2011 *Appl. Phys. Lett.* **98** 051904
[14] Schlom D G, Chen L Q, Eom C B, Rabe K M, Streiffer S K and Triscone J M 2007 *Annu. Rev. Mater. Res.* **37** 589
[15] Kleibeuker J E *et al* 2010 *Adv. Funct. Mater.* **20** 3490
[16] Ohtomo A and Hwang H Y 2004 *Nature* **427** 423
[17] Muller D A *et al* 2004 *Nature* **430** 657
[18] Choi K J *et al* 2004 *Science* **306** 1005
[19] Chen A *et al* 2011 *Adv. Funct. Mater.* **21** 2423
[20] Lee H N *et al* 2005 *Nature* **433** 395
[21] Chen A *et al* 2013 *Adv. Mater.* **25** 1028
[22] Rijnders G and Blank D H A 2005 *Nature* **433** 369
[23] Huijben M, Brinkman A, Koster G, Rijnders G, Hilgenkamp H and Blank D H A 2009 *Adv. Mater.* **2** 1665
[24] Thiel S, Hammerl G, Schmehl A, Schneider C W and Mannhart J 2006 *Science* **313** 1942
[25] Huijben M *et al* 2006 *Nature Mater.* **5** 556
[26] Pentcheva R *et al* 2010 *Phys. Rev. Lett.* **104** 166804
[27] Huijben M *et al* 2013 *Adv. Funct. Mater.* **23** 5240